ELASTIC-PLASTIC J-ANALYSIS FOR AN INNER SURFACE FLAW IN A PRESSURE VESSEL

W. Brocks*, H.-D. Noack*

Elastic-plastic finite element analyses of a pressurized cylinder with a deep inner surface flaw have been accomplished to study the effect of different loading conditions, i.e. axial forces and crack face loading. The local energy release rate was caculated by the method of virtual crack extension including a correction term if pressure acts on the crack faces. The numerical results are compared with different analytical assessments of J. Especially, a small scale yielding generalization of the Newman-Raju approximation is given, and a fully plastic solution for the maximum J is obtained by curve fitting of the FE results.

INTRODUCTION

The risk of failure of pressure vessels due to the presence of flaws is most commonly assessed by means of linear elastic fracture mechanics, e.g. in the ASME-Code (1). Since the first solution of Irwin (2) there have been numerous publications on the calculation of stress intensity factors for semi-elliptical surface flaws, for instance by Atluri and Kathiresan (3), (4), Kobayashi et al. (5), Mc Gowan and Raymund (6), Heliot et al. (7), Nishioka and Atluri (8). Newman and Raju (9), (10) established estimation formulas by fitting numerical results of their own and of various other authors, which work for different flaw shapes and vessel geometries.

Thus, the K-analysis of surface flaws is well established. Nevertheless, pressure vessels are usually operating at temperatures where the assumptions of linear elastic fracture mechanics in not met any more be-

* Bundesanstalt für Materialprüfung, Berlin

cause major plastic deformations will precede crack propagation. Hence, the J-integral or energy release rate has to replace the stress intensity factor K. As still no estimation formulas are available for an elastic-plastic J-analysis of surface flaws, expensive three-dimensional finite element calculations are necessary. The results of these calculations may then be taken to establish easier and less expensive methods of assessing J.

Aurich et al. (11) discussed the validity of a small scale yielding (ssy) approach

$$J_{ssy} = K^2_{eff}/E' = J(a_{eff}) \qquad (1)$$

introducing Irwin's idea of an "effective" crack length

$$a_{eff} = a + r_y, \qquad (2)$$

where r_y is the radius of the plastic zone, and an effective stress intensity factor which, in the case of $r_y \ll a$, becomes

$$K_{eff} = K\sqrt{a_{eff}/a}\ . \qquad (3)$$

As Irwin's model is a plane one its application to a three-dimensional structure and a curved crack front is non-trivial. It is one of the objectives of this paper to find a generalization for the variation of J along the crack front which bases on the Newman-Raju formula.

For large scale yielding, a plastic term has to be added to equation (1) which is a power function of (p/p_o) where p_o is some reference pressure whose significance will be discussed later

$$J = J_{ssy} + J_{pl}. \qquad (4)$$

A second objective is therefore to find an approximation formula for J_{pl} from elastic-plastic finite element (FE) calculations and to study the influence of different load boundary conditions, such as axial traction and crack face loading (cfl).

Only a stationary crack is considered here. Thus, the validity of the results ends as soon as stable crack growth has initiated.

FINITE ELEMENT MODEL AND J-ANALYSIS

The investigated cylindrical vessel has an inner radius (r_i) of 1400 mm and a wall thickness (t) of 140 mm, so that the ratio r_o/r_i = 1.10. Its total length is 3000 mm. Two deep inner surface flaws are supposed to be located along opposite axial lines, having a length (2c) of 480 mm and a depth (a) of 83 mm. Thus, we have a/t = 0.59 and a/c = 0.35.

Figure 1 shows the FE model of the vessel. Because of symmetry, only one eighth of the structure must be considered in the analysis. The mesh consists of 420 isoparametric 3 D elements and 1575 nodes total. Since the crack configuration was adapted to experimental fatigue cracks it has no ideal semi-elliptical shape as shown in Figure 2. Any point of the crack front is described by the parametric angle ϕ, which is 0° at the deepest point and ± 90° at the free surface, respectively.

The vessel is subjected to internal pressure (p) which has been increased up to yielding of the ligament. Three different boundary conditions are considered which will be referred to as Case A, B, C.

Case A (□) is the situation of an "open" tube with no external axial traction in z-direction; no crack face loading is considered, either.

Case B (x) represents a closed pressure vessel with domes causing an axial traction

$$p_z = p\, r_i^2 / (r_o^2 - r_i^2), \qquad (5)$$

but no crack face loading is considered.

Case C (Δ) accounts for pressure p acting on the crack faces as well as for actial traction p_z.

The program ADINA was used for the nonlinear FE analysis taking the elastic-plastic material model with the von Mises yield condition and isotropic hardening. The material stress-strain curve represents the German standard steel 20MnMoNi55 with a Young's modulus (E) of 210 000 MPa, a Poisson's ratio (ν) of 0.3, and a yield strength (σ_y) of 440 MPa, see reference (12). The analysis allows for large strains in the vicinity of the crack by using the updated Lagrangian formulation.

The local J-integral, $J(\phi)$, was calculated from the energy release rate due to a local virtual crack extension, $\delta a(\phi)$, see references (13) and (14). By this numerical method, the contour integral is transformed into a volume integral as proposed by Parks (15) and de Lorenzi (16). In case of crack face loading (cfl), an additional term of surface loads was included in order to reestablish path independency. Figure 4 shows for different pressures how the release rate is altered if FE domains of differing radius (r) around the crack tip are shifted. Additionally, the influence of the correction term for surface loads is plotted. In the following, the stationary value which is reached with increasing r will be taken as the local J value.

ELASTIC ANALYSIS

The stress intensity factor K results from the energy release rate by

$$K = \sqrt{J E'} \tag{6}$$

where

$$E' = \begin{cases} E & \text{for plane stress} \\ E/(1-\nu^2) & \text{for plane strain} \end{cases} \tag{7}$$

Plane strain condition was assumed for all $|\phi| < 90°$ and plane stress for $|\phi| = 90°$ at the surface. If we define the dimensionless magnification function

$$h_o(\phi) = \frac{K(\phi)}{\sigma_m \sqrt{\pi a/Q}\,(\sin^2\phi + (a/c)^2 \cos^2\phi)^{1/4}} \tag{8}$$

according to Irwin (2) we will obtain Figure 3 where the FE results are compared with solutions found in references (3), (6), (7), and (9). In equation (8), the membrane stress is defined by

$$\sigma_m = p\,(r_i/t), \tag{9}$$

and Q is the flaw shape parameter or square of the complete elliptical integral of second kind

$$\sqrt{Q} = \int_0^{\frac{\pi}{2}} \sqrt{1-(1-\frac{a^2}{c^2})\cos^2\phi}\; d\phi. \tag{10}$$

Whereas Newman and Raju (9) give an approximation formula which can be evaluated for arbitrary ratios of a/t and a/c, the remaining references are not quite comparable as they differ by the aspect ratios from the present flaw configuration. Apparently, the formula of Newman and Raju represents Case C, regarding cfl. No difference is found, of course, between Case A and

Case B because an axial traction must not influence the singularity at the crack tip for a linear elastic material. In addition, the linearity allows for a superposition of σ_m and p loading to easily obtain the influence of cfl on K . In fact, the $h_o(\phi)$ curve of Case C will collapse to that of Case A and Case B if we normalize it by $p\ (r_i/t + 1) = 1.1\ p$ instead of σ_m in equation (8). Thus, the influence of cfl on J is

$$J_{cfl} : J_{no\ cfl} = (1 + t/r_i)^2 \qquad (11)$$

ELASTIC PLASTIC ANALYSIS

Given the elastic solution we may obtain a small scale yielding (ssy) approximation for J by equation (1) to (3). Irwin gave an estimate for the extension of the plastic zone in the ligament ($2r_y$) derived from a simple 2 D model

$$2\ r_y = \frac{\beta}{\pi} \left(\frac{K}{\sigma_y}\right)^2 \qquad (12)$$

where

$$\beta = \begin{cases} (1-2\nu)^2 = 0.16 & \text{for plane strain} \\ 1 & \text{for plane stress} \end{cases} \qquad (13)$$

In Figure 5, these ssy solutions are compared with the maximum value of J at $\phi = 0°$ as obtained from the elastic plastic FE analyses. Additionally, the ASME Code (1) solution is plotted which includes a ssy correction via the flaw shape parameter, $Q(\sigma_m/\sigma_y)$, taking $\beta = 0.212$.

A 3D generalization of Irwin's model may be obtained by taking the local $K(\phi)$ for the surface flaw to calculate a local $r_y(\phi)$ provided that a realistic estimate of β is given. The real plastic zone size in a 3D structure will lie somewhere between the limits of plane strain and plane stress so that we expect $0.16<\beta<1.0$. We now assume that the ligament has fully yielded at $\phi = 0°$ if the plastic collapse pressure (p_F) according to Folias is reached:

$$2r_y = t-a \quad \text{if} \quad M\sigma_m = \sigma_y, \qquad (14)$$

M being the Folias factor, see reference (17). Introducing equation (8) we thus obtain

$$\beta_F = \frac{t-a}{a} \frac{M^2\ Q}{h_o^2} = 0.563. \qquad (15)$$

Figure 6 shows that this assumption for the plastic zone size agrees satisfactorily with the FE results as long as $p < p_F = 36.6$ MPa. The Newman and Raju formula was used to calculate $K(\phi)$ in equation (12).

A further assumption has to be made for the local crack depth $a(\phi)$ of the surface flaw which becomes clear from Figure 2. Finally we obtain

$$J_{ssy}(\phi) = \frac{1}{E'} K^2(\phi) \left[1 + \frac{\beta}{2\pi a(\phi)} \left(\frac{K(\phi)}{\sigma_Y}\right)^2\right] \qquad (16)$$

which is plotted in Figure 7 and, again, agrees well with the elastic plastic FE results though the yielded zone is by no means "small" at $p = 35$ MPa.

If the pressure p equals or exceeds the plastic limit the ssy approach is not adequate any more and equation (4) must be used for assessing J. The fully plastic solution is given by

$$J_{pl} = J_o \left(\frac{p}{p_o}\right)^m \qquad (17)$$

where, usually, the plastic limit load is taken as the reference pressure p_o, see reference (18). We set $p_{oA} = p_F = 36.6$ MPa for Case A, and expect that, due to a higher triaxiality of the stress state induced by axial tension,

$$p_{oC} \approx p_{oB} > p_{oA} = p_F \qquad (18)$$

which is confirmed by the FE calculations where ligament yielding was reached at 35, 40, and 40 MPa in Case A, B, and C, respectively.

As no further indications to the fully plastic solution could be found, the coefficients of equation (17) were determined by curve fitting of the FE results. Only the maximum J at $\phi = 0°$ is considered here and J_{ssy} in equation (4) was calculated from Irwin's plane strain solution. The resulting data are summarized in Table 1 and the total J which follows from equation (4) and (17) is plotted in Figure 8. The coefficients J_o and m do not depend on axial traction but on crack face loading and, thus, appear not to be material constants. The exponent m is about twice the Ramberg-Osgood hardening exponent n which ranges between 5 and 7 for the considered material, see reference (12).

TABLE 1 - Coefficients of the fully plastic solution of J at $\phi = 0°$ as obtained by curve fitting

CASE	p_o (MPa)	J_o (N/mm)	m
A	36.6	51.9	10
B	39.3	51.9	10
C	41.6	161.4	13

SYMBOLS USED

a = depth of surface crack (minor principal axis)

c = half-length of surface crack (major principal axis)

ϕ = parametric angle of the ellipse

Q = shape factor for an elliptical crack

t = wall thickness of vessel

r = radius, half-diameter

p = pressure

E = Young's modulus

ν = Poisson's ratio

σ = stress

K = stress intensity factor (Mode I)

J = J-integral

subscripts and abbreviations

i = inner

o = outer (radius) or reference (pressure)

eff = effective

el = elastic

pl = plastic

y = yield

ssy = small scale yielding

cfl = crack face loading

ACKNOWLEDGEMENT

The results reported herein were obtained during the course of investigations supported by the Bundesminister für Forschung und Technologie of the Federal Republic of Germany.

REFERENCES

(1) ASME Boiler and Pressure Vessel Code, Section XI, Appendix A.

(2) Irwin, G. R., J. Appl. Mech., Vol. 29, 1962, pp. 651 - 654.

(3) Atluri, S. N. and Kathiresan, K., Trans. 5th SMiRT, Berlin, Germany, 1979, paper G4/3.

(4) Atluri, S. N. and Kathiresan, K., Nucl. Eng. and Design, Vol. 51, 1979, pp. 163 - 176.

(5) Kobayashi, A. S., Emery, A. F., Love, W. J. and Jain, A., Trans. 5th SMiRT, Berlin, Germany, paper G4/1.

(6) Mc Gowan, J. J. and Raymund, M., STP 677, ASTM, Philadelphia, USA, 1979, pp. 365 - 380.

(7) Heliot, J., Labbens, R. C. and Pelissier-Tanon, A., STP 677, ASTM, Philadelphia, USA, 1979, pp. 341 - 364.

(8) Nishioka, T. and Atluri, S. N., Trans. ASME, J. Pressure Vessel Technology, Vol. 104, 1982, pp. 299 - 307.

(9) Newman, J. C. and Raju, I. S., Trans. 5th SMiRT, Berlin, Germany, 1979, paper G7/3.

(10) Raju, I. S. and Newman, J. C., Trans. ASME, J. Pressure Vessel Technology, Vol. 104, 1982, pp. 293 - 298.

(11) Aurich, D., Brocks, W., Noack, H.-D. and Veith, H., STTP 868, ASTM, Philadelphia, USA, 1985, pp. 617 - 631.

(12) Brocks, W. and Olschewski, J., Proc. 6th ECF, Amsterdam, the Netherlands, 1986.

(13) Bakker, A., "The Three-Dimensional J-Integral", report WTHD No. 167, Dep. of Mech. Engng., Delft University of Technology, the Netherlands, 1984.

(14) Matzkows, J., Boddenberg, R. and Kaiser, F., "Programm JINFEM, Postprozessor für das Programm ADINA", Report Hb-18-030, IWiS GmbH, Berlin, Germany, 1985.

(15) Parks, D. M., Proc. 1st Int. Conf. Numerical Methods in Fracture Mechanics, Swansea, UK, 1978, pp. 464 - 478.

(16) de Lorenzi, H. G., Int. J. Fracture, Vol. 19, 1982, pp. 183 - 192.

(17) Schulze, H. D., Togler, G. and Bodmann, E., Nucl. Eng. and Design, Vol. 58, 1980, pp. 19 - 31.

(18) Kumar, V. et al., "Advances in Elastic-Plastic Fracture Analysis", NP-3607, Research Projekt 1237-1, EPRI, Palo Alto, California, USA, 1984.

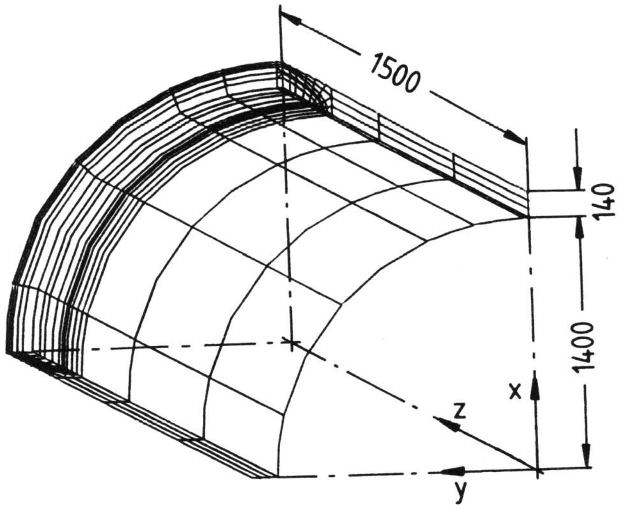

Figure 1 Finite element model of the pressure vessel

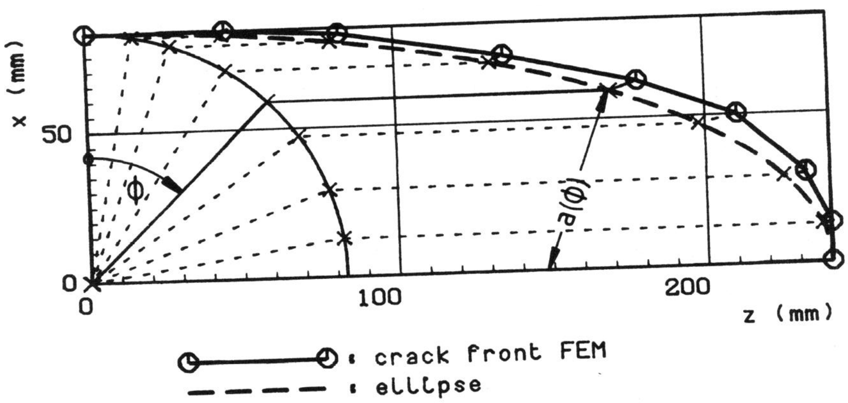

Figure 2 Geometry of the semi-elliptical surface flaw and definition of parametric angle ϕ

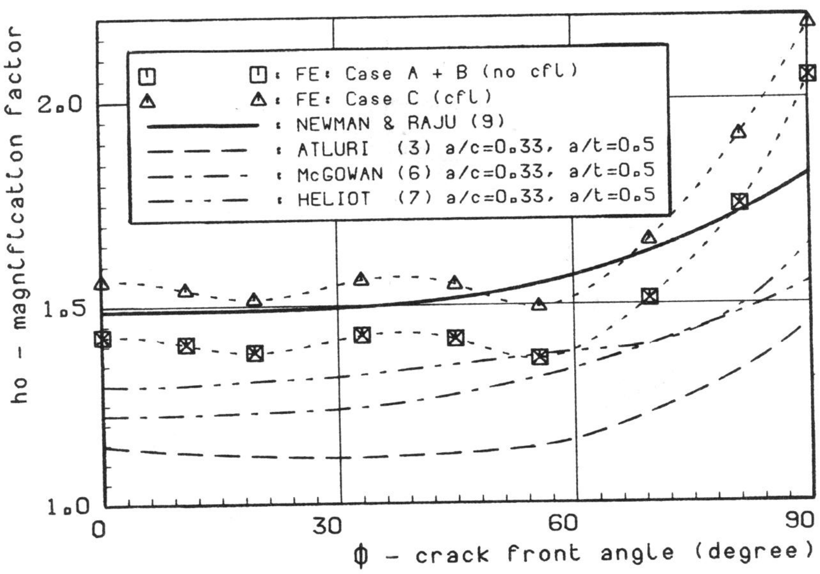

Figure 3 Magnification factor for stress intensity (elastic solution)

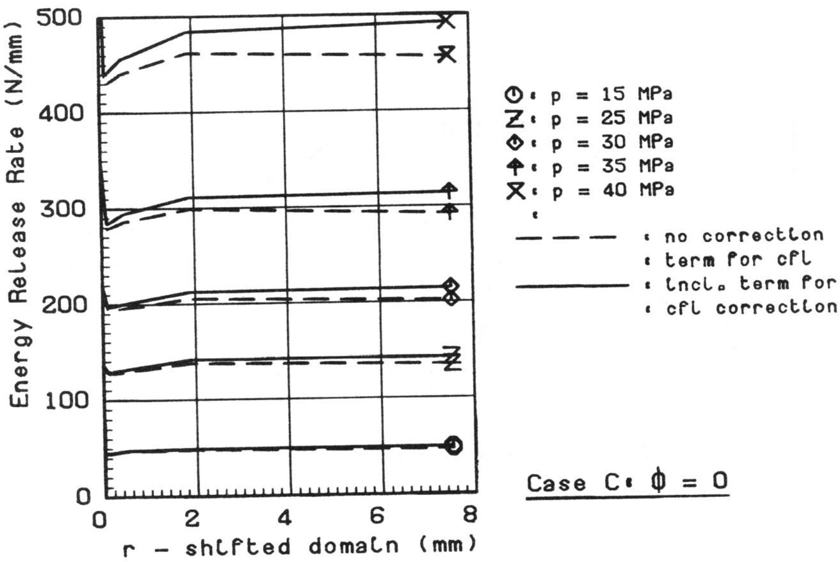

Figure 4 Virtual crack extension method, path dependency of energy release rate

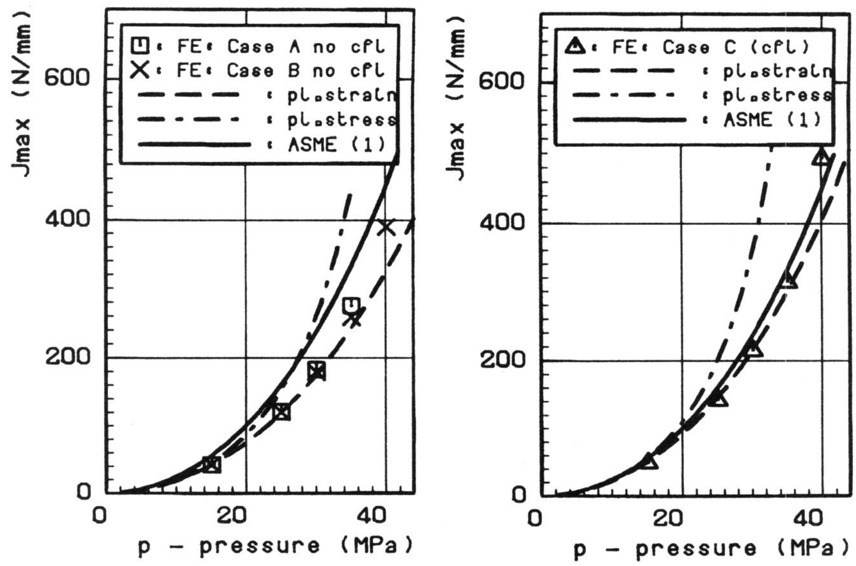

Figure 5 J-integral at ϕ = 0°, FE results and Irwin's analytical ssy solutions

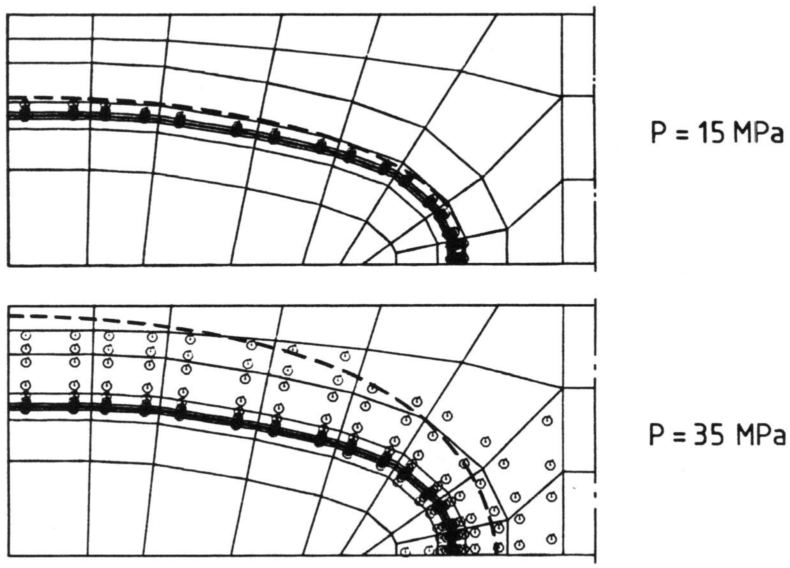

Figure 6 Plastic zones in the crack plane, FE results (⊙) and 3D ssy model (– – –)

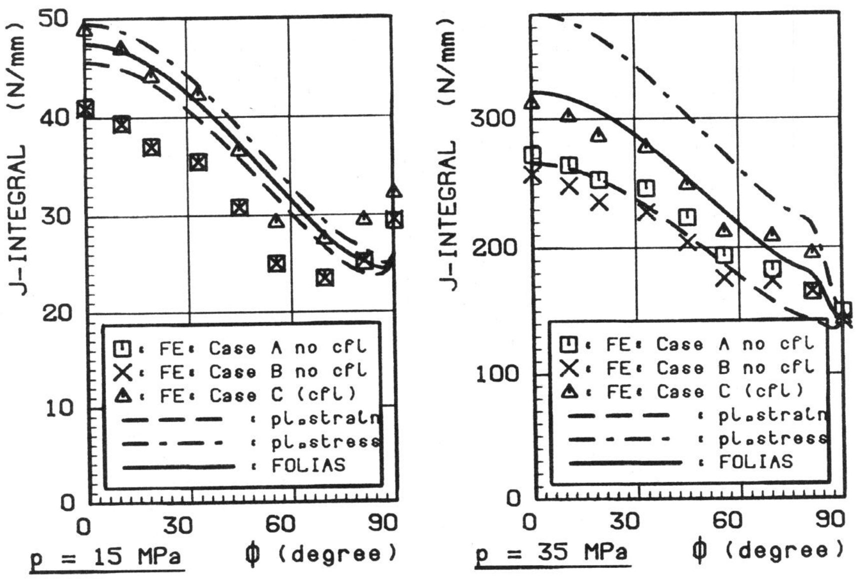

Figure 7 Variation of J along the crack front, FE results and ssy solutions

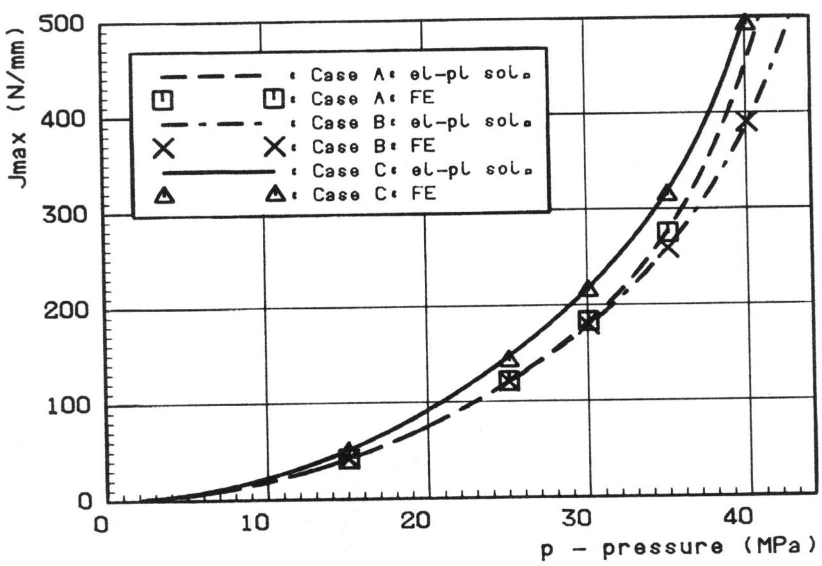

Figure 8 J-integral at ϕ = 0°, FE results and fitted elastic-plastic solution